European Journal of Pharmaceutics and Biopharmaceutics 71 (2009) 196–206

Contents lists available at ScienceDirect

European Journal of Pharmaceutics and Biopharmaceutics

journal homepage: www.elsevier.com/locate/ejpb

Research paper

In vitro human plasma distribution of nanoparticulate paclitaxel is dependent on the physicochemical properties of poly(ethylene glycol) -block-poly(caprolactone) nanoparticles

Kevin Letchford [a], Richard Liggins [b], Kishor M. Wasan [a], Helen Burt [a,*]

[a] Faculty of Pharmaceutical Sciences, University of British Columbia, Vancouver, BC, Canada
[b] Centre for Drug Research and Development, University of British Columbia, Vancouver, BC, Canada

ARTICLE INFO

Article history:
Received 13 May 2008
Accepted in revised form 7 August 2008
Available online 15 August 2008

Keywords:
Micelle
Nanosphere
Nanoparticle
Paclitaxel
Amphiphilic block copolymer
Plasma distribution
Hemocompatibility

ABSTRACT

In this study, we synthesized and characterized two methoxy poly(ethylene glycol)-block-poly(caprolactone) (MePEG-b-PCL) amphiphilic diblock copolymers, both based on MePEG with a molecular weight of 5000 g/mol (114 repeat units) and PCL block lengths of either 19 or 104 repeat units. Nanoparticles were formed from these copolymers by a nanoprecipitation and dialysis technique. The $MePEG_{114}$-b-PCL_{19} copolymer was water soluble and formed micelles that had a hydrodynamic diameter of 40 nm at all copolymer concentrations tested, and displayed a relatively low core microviscosity. The practically water insoluble $MePEG_{114}$-b-PCL_{104} copolymer formed nanoparticles with a larger hydrodynamic diameter, which was dependent on copolymer concentration, and possessed a higher core microviscosity than the $MePEG_{114}$-b-PCL_{19} micelles, characteristic of nanospheres. The micelles solubilized a maximum of 1.6% w/w of the hydrophobic anticancer agent, paclitaxel (PTX), and released 92% of their drug payload over 7 days, as compared to the nanospheres, which solubilized a maximum of 3% w/w of PTX and released 60% over the same period of time. Both types of nanoparticles were found to be hemocompatible, causing only minimal hemolysis and no changes in plasma coagulation times as compared to control. Upon *in vitro* incubation in human plasma, PTX solubilized by micelles had a plasma distribution similar to free drug. The majority of PTX was associated with the lipoprotein deficient plasma (LPDP) fraction, which primarily consists of albumin and alpha-1glycoprotein. In contrast, nanospheres were capable of retaining more of the encapsulated drug with significantly less PTX partitioning into the LPDP fraction.
© 2008 Elsevier B.V. All rights reserved.

1. Introduction

The use of amphiphilic block copolymers for the formation of nanoparticulate drug delivery vehicles for hydrophobic compounds has been investigated for more than a decade [1,2]. In an aqueous environment these materials form nano-sized structures possessing a core–shell morphology which is characterized by a hydrophobic core surrounded by a highly water bound, hydrophilic corona. A variety of core forming blocks have been evaluated; however, the most common choices are biodegradable and biocompatible polyesters such as poly(D,L lactic acid) (PDLLA) [3], poly(caprolactone) (PCL) [4], or poly(lactic-co-glycolic acid) (PLGA) [5]. The hydrophobic core has been utilized as a cargo space for poorly water-soluble drugs, increasing their aqueous solubility and providing controlled release. Typically, the hydrophilic block is poly(ethylene glycol) (PEG) or methoxy poly(ethylene glycol) (MePEG). A PEG coating on the surface of nanoparticles acts to reduce the adsorption of plasma proteins such as opsonins and apolipoproteins on the surface of nanoparticles. This prevents the particle's recognition by the mononuclear phagocytes system, prolonging the circulation of PEGylated nanoparticles in blood [6,7]. PEG coated nanoparticles can also resist adsorption of proteins of the coagulation cascade thus preventing thrombosis [8]. These shielding effects require sufficient PEG chain length and density at the surface of the particles to effectively repel plasma proteins [7].

Amphiphilic block copolymer nanoparticles can be categorized in terms of structure as micelles, nanospheres, crew-cut micelles, and polymersomes. The type of structure formed is dependent on the relative lengths of the hydrophobic and hydrophilic blocks of the copolymer, molecular weight, as well as on the method of preparation (see [9] for review). Although micelles and nanospheres both have a core–shell architecture, they differ in a few fundamental ways. The copolymer chains of micelles, formed from water soluble amphiphilic copolymers, are in a dynamic equilib-

* Corresponding author. Faculty of Pharmaceutical Sciences, University of British Columbia, 2146 East Mall, Vancouver, BC, Canada V6T 1Z3. Tel.: +1 604 822 2440; fax: +1 604 822 3035.
E-mail address: burt@interchange.ubc.ca (H. Burt).

0939-6411/$ - see front matter © 2008 Elsevier B.V. All rights reserved.
doi:10.1016/j.ejpb.2008.08.003

rium with free unimers in solution [10] and therefore, should not be considered solid particles, but rather association colloids [11]. As the length of the hydrophobic block increases, the copolymer becomes water insoluble. In order to form nanoparticles from these relatively hydrophobic copolymers, they must first be solubilized in an organic solvent prior to emulsification or precipitation. The resulting structures exhibit a core–shell architecture similar to micelles, but are generally larger and possess a more solid-like core and are considered to be a separate phase [12]. These nanoparticles are termed nanospheres.

Studies in which doxorubicin loaded amphiphilic copolymer nanoparticles have been administered intravenously in animal models have shown that some formulations increased circulation time and plasma half-life, altered tissue distribution and in the case of tumour models, resulted in passive targeting to tumours via the enhanced permeation and retention effect [1,13–15]. Nanoparticulate formulations for the anticancer drug paclitaxel have also been investigated in order to improve its water solubility and toxicity profile. Paclitaxel is commercially formulated in a mixture of Cremophor® EL and ethanol as Taxol™. Unfortunately, Cremophor® EL has been attributed to hypersensitivity reactions [16] and so there has been a strong effort to find a replacement for this excipient. Copolymer micellar formulations have been shown to readily solubilize PTX and were better tolerated than Taxol™, resulting in an increased maximum tolerated dose. These formulations have demonstrated improved efficacy against several cancer cell lines compared to Taxol™ due to the ability to administer a higher dose of Taxol™ [17–19]. Although there have been a few studies in which the pharmacokinetics and biodistribution of micellar PTX were improved over the commercially available product [20,21], *in vivo* evaluations of several other micellar PTX formulations have shown little benefit over Taxol™, with respect to prolonging drug circulation time and increasing tumour uptake [18,22,23]. Our group has compared the *in vitro* distribution of PTX solubilized in MePEG-b-PDLLA micelles and free PTX into the component fractions of plasma. Both free and micellized PTX rapidly distributed into lipoprotein and lipoprotein deficient plasma fractions suggesting that the drug was released from the micelles and associated with the plasma proteins [24]. Pharmacokinetic studies of non-drug loaded diblock copolymer micelles have shown that copolymer nanoparticles are capable of prolonged circulation in the blood [25,26]; however, in many cases it is apparent that PTX does not remain with the carrier. It is evident that in order to increase the blood circulation time of PTX, better drug retention within the nanoparticle core is necessary. Several methods to retain PTX in the nanoparticle core have been investigated including cross-linking the hydrophobic blocks [27,28], conjugating the drug to the core forming block [29] and altering the structure of PTX so that it is more compatible with the micelle core [30]. It has also been suggested that increasing the hydrophobic block length may retain the drug for a longer period of time by increasing thermodynamic and kinetic stability of the nanoparticle as well as prolonging the release of the drug [31].

Although it has been suggested that there are differences in the physicochemical properties of micelles and nanospheres, such as mobility of the core blocks and thermodynamic and kinetic stabilities, there has not been a comparison of how these two types of nanoparticles interact with blood and plasma constituents or how the encapsulated drug distributes into plasma fractions [32,33]. Given the administration of drug loaded nanoparticles directly into the blood, it is also critical to understand the hemocompatibilities of these nanoparticles. In this work, two methoxy poly(ethylene glycol)-block-poly(caprolactone) (MePEG-b-PCL) amphiphilic diblock copolymers, one with a short PCL block (micelle-forming) and the other with a long PCL block (solid-like core, nanosphere-forming), were used to elucidate the interactions of micelles and nanospheres with plasma components. Micelles and nanospheres were characterized with respect to their hydrodynamic diameters, core microviscosities, and solubilization and *in vitro* release of PTX. These physicochemical characteristics were related to the differences in their hemocompatibility, as assessed by measuring coagulation times and the rate of hemolysis, as well as differences in the *in vitro* plasma distribution of PTX solubilized by these two nanoparticulate delivery systems.

2. Experimental methods

2.1. Materials

Methoxy poly(ethylene glycol) (MePEG) (Fluka, Bucks SG, Switzerland), ε-caprolactone (Fluka), stannous octoate (Sigma–Aldrich Canada Ltd, Oakville, Ont.), 1,6-diphenyl-1,3,5-hexatriene (Sigma–Aldrich Canada Ltd), sphingomyelin (Sigma–Aldrich Canada Ltd), *N*,*N*,-dimethyl formamide (Fisher Scientific Co., Ottawa, Ont.), paclitaxel (Polymed Therapeutics Inc., Houston, TX), polysorbate 20 (Sigma–Aldrich Canada Ltd), and Triton X-100 (Sigma–Aldrich Canada Ltd) were used as supplied without further purification. The solvents chloroform (Fisher Scientific Co., HPLC grade), deuterated chloroform (Cambridge Isotope Laboratories, Andover, MA), acetonitrile (Fisher Scientific Co., HPLC grade), ethanol (Fisher Scientific Co., HPLC grade), and methanol (Fisher Scientific Co., HPLC grade) were also used as supplied.

2.2. Synthesis and characterization of MePEG-b-PCL diblock copolymers

Two copolymers were synthesized and characterized using methods previously described [34–36]. Briefly, methoxy terminated poly(ethylene glycol) (MePEG) with a molecular weight of 5000 g/mol was combined with ε-caprolactone in weight ratios of either 30:70 or 70:30 with a total mass of 50 g. The reagents were reacted at 140 °C for 24 h in a sealed round-bottomed flask using 0.15 ml of stannous octoate as a catalyst. The copolymer molecular weight was determined by gel permeation chromatography (GPC) against poly(ethylene glycol) standards (Polymer Laboratories Inc., Amherst, MA) in the range of 670–22,800 g/mol using chloroform as a mobile phase with a flow rate of 1 ml/min. Samples were injected using a Waters (Milford, MA) model 717 plus autosampler, and separation was achieved through two Waters Styragel columns (HR 3 and HR 1) connected in series. Detection was through a Waters model 2410 refractive index detector with a cell temperature of 40 °C. The compositions of the copolymers were determined by proton NMR spectra of 10% w/v solutions of the copolymers in deuterated chloroform. The spectra obtained from a 400-MHz NMR instrument (Bruker Bio Spin Corp., Billerica, CA) were analyzed using MestRe-C 2.3a software. The peaks situated around 1.3 and 1.55 ppm from the caprolactone methylene protons and the peaks at 3.55 ppm from the MePEG methylene protons were used to calculate the degree of polymerization (DPn).

2.3. Formation and characterization of MePEG-b-PCL nanoparticles

Nanoparticles were formed by a nanoprecipitation technique. Briefly, 0.5 ml copolymer solutions were prepared in *N*,*N*,-dimethyl formamide (DMF) at concentrations ranging from 15 to 240 mg/ml. This solution was added drop-wise to 2.5 ml of rapidly stirring PBS (0.01 M, pH 7.4). The DMF was removed from the solution by dialysis in PBS overnight using 3500 MWCO Spectra/Por® dialysis membranes (Spectrum Laboratories, Inc., Rancho Dominguez, CA). For the drug loading, release and plasma distribution experiments, the resulting dialysate was diluted with PBS so that the final copolymer concentration was 0.36 mM.

The hydrodynamic diameter of nanoparticles was determined by light scattering measurements carried out on a Malvern 3000HS Zetasizer (Malvern Instruments Ltd, Malvern, UK) with a He–Ne laser (532 nm) and 90° collecting optics. Measurements were made at 37 °C on copolymer samples at concentrations ranging from 15 to 240 mg/ml of copolymer in the initial DMF solution. Data were analyzed using CONTIN algorithms provided by Malvern Zetasizer software.

Cryogenic transmission electron microscopy (cryo TEM) was carried out by Dr. Göran Karlsson at Uppsala University. Nanoparticles were prepared in distilled water at a copolymer concentration of 0.36 mM as previously described. Samples were equilibrated at 25 °C and 99% relative humidity in a climate chamber prior to sample preparation. Copper grids (Agar Scientific, Essex, England) were covered with a perforated cellulose acetate butyrate film (Aldrich-Chemie, Steinheim, Germany) and a thin coating of carbon. A small amount of sample (<1 μl) was deposited on the grid followed by blotting with filter paper to leave a thin film on the grid. The grid was then vitrified in liquid ethane, held just above its freezing point of –182 °C. A Zeiss EM 902A Transmission Electron Microscope (Carl Zeiss NTS, Oberkochen, Germany) was used to image the samples. The instrument was operated at 80 kV and in zero loss bright-field mode. Digital images were recorded under low dose conditions with a BioVision Pro-SM Slow Scan CCD camera (Proscan GmbH, Scheuring, Germany) and iTEM software (Soft Imaging System, GmbH, Münster, Germany).

To investigate the differences in the microviscosity of the nanoparticle cores, the MePEG-b-PCL nanoparticles were loaded with the fluorescent probe 1,6-diphenyl-1,3,5-hexatriene (DPH) by adding 4.2 μL of a 2-μM solution in chloroform to the nanoparticle solution in amber glass vials. The probe was allowed to partition into the nanoparticle core overnight with stirring. For comparison, polysorbate 20 micelles were prepared by diluting polysorbate 20 in PBS so that the final surfactant concentration was 6 mg/ml. Similar to the MeEPG-b-PCL nanoparticles, DPH was partitioned into polysorbate 20 micelles overnight with stirring. As a positive control DPH was solubilized in a sphingomyelin bilayer. Sphingomyelin in chloroform and the stock DPH solution were added to an amber glass vial and the solvent was evaporated under nitrogen gas to form a thin film. Warm PBS was added to the vial and the film was dissolved by vortexing and sonicating so that the final sphinomyelin concentration was 6 mg/ml. For all samples the fluorescent intensity of DPH was measured parallel (Ivv) and perpendicular (Ivh) to vertically polarized light over the temperature range of 27–61 °C using a Varian Cary Eclipse fluorescence spectrophotometer (Varian Inc., Palo Alto, CA). Excitation and emission wavelengths were 365 and 428 nm, respectively. The fluorescence anisotropy (r) was calculated as

$$r = \frac{\mathrm{Ivv} - \mathrm{Ivh}}{\mathrm{Ivv} + 2\mathrm{Ivh}}. \quad (1)$$

To determine the maximum loading of PTX in the nanoparticles, several nanoparticle solutions were prepared with increasing amounts of drug in the DMF/copolymer solution. After dialysis, the dialysate was centrifuged at 14,000 rpm to remove any precipitate, and an aliquot of the nanoparticle solution was dried under a stream of nitrogen gas and reconstituted in acetonitrile. This solution was analyzed for PTX content by HPLC as described elsewhere [37]. The loading efficiency of the nanoparticles was calculated as

$$\text{Loading efficiency} = \frac{[\mathrm{PTX}]_{\mathrm{solubilized}}}{[\mathrm{PTX}]_{\mathrm{added}}} \times 100, \quad (2)$$

where $[\mathrm{PTX}]_{\mathrm{solubilized}}$ is the concentration of PTX found in solution after encapsulation in nanoparticles as determined by HPLC and $[\mathrm{PTX}]_{\mathrm{added}}$ is the concentration of PTX added to the solution during the formation of nanoparticles. The hydrodynamic diameter of the nanoparticles at the maximum PTX loading was determined by DLS as described above.

2.4. In vitro paclitaxel release

Nanoparticles with a copolymer concentration of 0.36 mM were loaded with PTX as described above, with the exception that a small amount of ^{3}H PTX was added to the drug/copolymer solution prior to dialysis. The initial cold PTX loading of nanoparticles was 40 μg/ml. Loaded nanoparticle solutions (3 ml) were added to 6000–8000 MWCO dialysis bags (Spectrum Laboratories, Inc., Rancho Dominguez, CA) and dialysed against 500 ml of PBS at 37 °C with shaking at 75 rpm. As a control, 3 ml of PBS in a dialysis bag was spiked with an aliquot of cold PTX in ethanol containing a trace amount of ^{3}H PTX so that the resulting drug concentration was 1 μg/ml, equivalent to the aqueous solubility of PTX. At time points of 0, 2, 4, 8, and 12 h and 1, 2, 4, and 7 days, the volumes of the dialysis bags were measured and a 10 μl sample was taken for measurement of the remaining ^{3}H PTX in the dialysis bags. At each time point the entire external release media was exchanged with fresh PBS. The concentration of ^{3}H PTX remaining in the dialysis bag at each time point was determined by beta scintillation counting (Beckman Coulter Canada, Mississagua, ON). The cumulative percent drug released was calculated by subtracting the amount of drug remaining from the initial amount of drug in the dialysis bag at the beginning of the experiment. The data were expressed as cumulative percentage of drug released as a function of time.

2.5. Blood compatibility and plasma partitioning

2.5.1. Plasma clotting

Blood was collected from a healthy human volunteer (according to protocols approved by UBC Clinical Research Ethics Board) in an evacuated siliconized glass tube containing 3.2% sodium citrate. Platelet poor plasma was isolated from the blood sample by centrifuging at 2000g for 15 min at room temperature. A coagulation analyzer with mechanical endpoint determination (ST4 Diagnostica, Stago) was used to analyze prothrombin time (PT) and activated partial thromboplastin time (APTT). Nanoparticle solutions with varying concentrations were added to the plasma samples in a 1:1 ratio and mixed at room temperature so that the final copolymer concentration varied from 0.0036 to 0.36 mM. For the PT determination, Innovin® reagent (Dade Behring) was added to the sample, whereas for APTT, partial thromboplastin reagent, Actin® (Dade Berhing) was added along with calcium chloride. Controls consisted of identical volumes of PBS added to the plasma. Results were analyzed for statistical significance using an ANOVA. Differences were considered significant at $p < 0.05$. A Neuman–Keuls post hoc test was performed when a difference was detected.

2.5.2. Hemolysis

Blood was collected from a healthy human volunteer in an evacuated siliconized glass tube containing sodium heparin. To separate red blood cells, the sample was centrifuged at 2000 rpm for 10 min, and 1 ml of the packed cells was removed and washed three times with PBS. A stock suspension of erythrocytes in PBS was prepared so that the cell count was 1×10^8 cells/ml. Nanoparticle dispersions at 0.02%, 0.1%, and 0.2% w/v were prepared by nanoprecipitation as described above. As a positive control, micelles of a copolymer that has previously been shown to cause hemolysis, MePEG_{17}-b-PCL_4 [38], were prepared by direct dissolution of the copolymer in 37 °C PBS at the concentrations mentioned above. An equal volume of erythrocyte suspension and nanoparticle solution was combined in a microcentrifuge tube so that the final erythrocyte concentration was 5×10^7 cells/ml and the final

copolymer concentration was 0.1%, 0.05% or 0.01% w/v. A spontaneous hemolysis control was prepared by incubation of erythrocytes with PBS, also in a 1:1 ratio. A 100% hemolysis control was prepared by the addition of an equal volume of erythrocyte suspension and 1% Triton X-100. All tubes were incubated at 37 °C with tumbling. At time intervals of 1, 6 and 12 h the tubes were centrifuged at 20,000*g* for 15 s and the hemoglobin released in the supernatant was detected by UV absorbance at 540 nm (Cary Bio 50 UV Visible spectrophotometer, Varian). The percent hemolysis was calculated by

$$\%\text{Hemolysis} = \frac{(\text{Abs}_{\text{sample}} - \text{Abs}_{\text{spontaneous}})}{\text{Abs}_{100\%\text{hemolysis}}} \times 100, \quad (3)$$

where $\text{Abs}_{\text{sample}}$ is the absorbance of the supernatant of the erythrocyte and nanoparticle suspension, $\text{Abs}_{\text{spontaneous}}$ is the absorbance of the supernatant of the erythrocyte and PBS suspension and $\text{Abs}_{100\%\text{hemolysis}}$ is the absorbance of the supernatant of the erythrocyte and Triton X-100 solution. Due to the opalescent appearance of the nanosphere dispersions at higher concentrations, the maximum copolymer concentration was 0.1% w/v to minimize the amount of background absorbance at 540 nm.

2.5.3. PTX plasma distribution

Nanoparticle solutions were prepared with a polymer concentration of 0.36 mM and a loading of 40 μg/ml of cold PTX along with a trace amount of ^{3}H PTX as described above. An aliquot of these solutions or free PTX with a trace amount of ^{3}H PTX was added to human plasma (Bioreclamation Inc., Hicksville, NY) so that the final PTX concentration in plasma was 6.7 μg/ml. The samples were incubated for either 1, 6, 12, or 24 h at 37 °C with shaking at 75 rpm. After the specified incubation period, 1 ml of plasma was removed for comparison. Into the remaining 3 ml, 1.02 g of NaBr was dissolved to adjust the density of the plasma to 1.25 g/ml, and the plasma was cooled at 4 °C for 2 h to prevent any further drug redistribution. The plasma was then separated into its lipoprotein and lipoprotein deficient fractions by density gradient ultracentrifugation as described elsewhere [39]. Briefly, onto the plasma, sodium bromide solutions with densities of 1.21, 1.063, and 1.006 g/ml were layered, representing the high density lipoprotein (HDL) fraction, low density lipoprotein (LDL) fraction and very low density lipoprotein/chylomicron (VLDL) fractions, respectively. The solutions were centrifuged for 18 h at 40,000 rpm (288,000*g*) in SW41 Ti swinging buckets at 15 °C (Beckman Coulter, Fullerton, CA). Immediately after centrifugation, the layers were removed and the volumes measured. The amount of ^{3}H PTX in each fraction was quantified by beta scintillation counting and the amount of drug expressed as a percentage of total ^{3}H PTX as determined by the 1 ml of plasma removed prior to centrifugation. In order to determine whether the partitioning of the drug was due to interactions with plasma components and not due to the density of the formulation, plasma free controls were run. For these controls, the same experiment was run as described above, except the drug loaded nanoparticles or free PTX were incubated for 1 h in distilled water (in place of plasma). Results were analyzed for statistical significance using an ANOVA. Differences were considered significant at $p < 0.05$. A Neuman–Keuls post hoc test was performed when a difference was detected.

3. Results

3.1. Synthesis and characterization of MePEG-b-PCL diblock copolymers

Two MePEG-b-PCL diblock copolymers both with MePEG molecular weights of 5000 g/mol but different PCL molecular weights were synthesized by a ring opening mechanism of caprolactone using the hydroxyl terminus of MePEG as the initiator. By varying the ratio of MePEG:PCL in the reaction mixture, the final composition of the copolymer was controlled. As previously reported, the degree of polymerization (DPn) and hence the number of repeat units of caprolactone were determined by ^{1}H NMR [34]. The multiplet at 3.55 ppm was assigned to the methylene groups of MePEG, and the sum of the integrated peaks at 1.5 and 1.3 ppm was assigned to the methylene protons of the caprolactone repeat unit.

3.2. Formation and characterization of MePEG-b-PCL nanoparticles

In order to eliminate the potential influence of different methods of preparation on the properties of the nanoparticles, the method of nanoprecipitation was used for both copolymers. The nanoparticulate dispersions formed by the two copolymers differed in appearance. Upon visual inspection, the MePEG_{114}-b-PCL_{104} dispersion was opalescent in appearance, becoming increasingly turbid with concentration, while the MePEG_{114}-b-PCL_{19} dispersion was clear and one phase over the range of copolymer concentrations tested. The diameters of the nanoparticles were determined by light scattering. Both types of nanoparticles had monodisperse distributions. The average hydrodynamic diameter of nanoparticles composed of MePEG_{114}-b-PCL_{19} remained constant at approximately 40 nm over all concentrations tested, whereas those composed of MePEG_{114}-b-PCL_{104} increased dramatically as the concentration of copolymer in the initial DMF solution increased, ranging from 73 to 135 nm over a copolymer concentration range of 15–180 mg/ml (Fig. 1). Inspection of the cryo TEM images revealed spherical particles; however, the diameters of the particles were smaller than that determined by DLS, particularly for the MePEG_{114}-b-PCL_{19} micelles (Fig. 2).

Fluorescence anisotropy was used to investigate the differences in the core microviscosity of nanoparticles formed from either MePEG_{114}-b-PCL_{104} or MePEG_{114}-b-PCL_{19} (Fig. 3). The hydrophobic fluorescence probe, DPH, is sensitive to the microviscosity of its surroundings and displays changes in its depolarization as measured by fluorescence anisotropy. As a positive control, DPH was solubilized in a sphingomyelin bilayer. Upon heating the sphinomyelin, the anisotropy dropped significantly between 35 and 45 °C. Both copolymer nanoparticles displayed a decrease in the anisotropy implying a decrease in the microviscosity of the core during heating. However, those composed of MePEG_{114}-b-PCL_{104} had higher anisotropy values than those composed of MePEG_{114}-b-PCL_{19} over all temperature ranges. As a comparison, DPH was

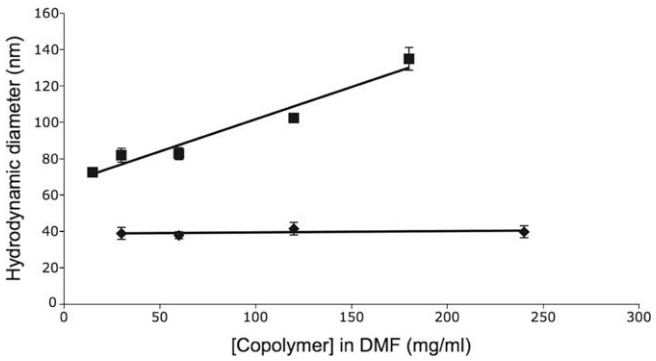

Fig. 1. Dependence of nanoparticle hydrodynamic diameter on copolymer concentration. MePEG_{114}-b-PCL_{19} micelles and (■) MePEG_{114}-b-PCL_{104} nanospheres (♦). All points represent the mean hydrodynamic diameter ± SD ($n = 3$).

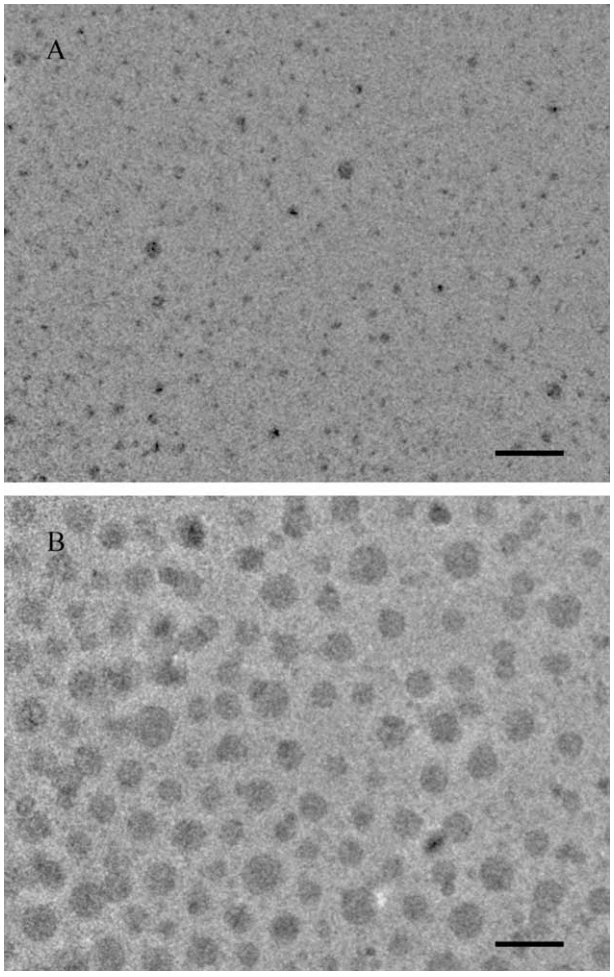

Fig. 2. Cryo TEM images of (A) $MePEG_{114}$-b-PCL_{19} micelles and (B) $MePEG_{114}$-b-PCL_{104} nanospheres. Bar represents 100 nm.

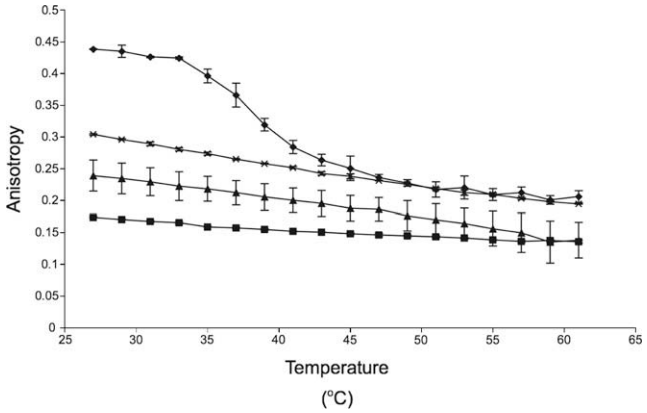

Fig. 3. Anisotropy as a function of temperature. Spingomyelin bilayer (♦) $MePEG_{114}$-b-PCL_{19} micelles (▲) $MePEG_{114}$-b-PCL_{104} nanospheres (×) polysorbate 20 micelles (■). All points represent the mean anisotropy value ± SD (n = 3).

solubilized in polysarbate 20 micelles. Anisotropy values lower than those of $MePEG_{114}$-b-PCL_{19} were found over all temperatures for polysorbate 20.

The solubilization capacity of PTX in nanoparticulate dispersions of each of the synthesized copolymers was investigated (Fig. 4). In these experiments, each copolymer at a concentration of 0.36 mM was used to solubilize increasing amounts of drug.

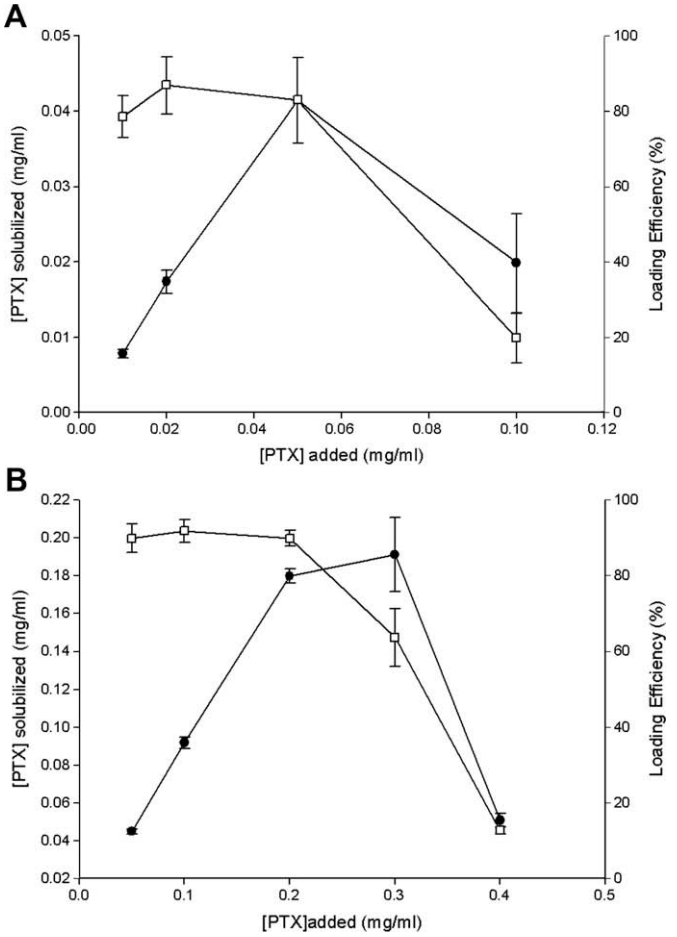

Fig. 4. Solubilization of PTX by (A) $MePEG_{114}$-b-PCL_{19} micelles and (B) $MePEG_{114}$-b-PCL_{104} nanospheres formed by nanoprecipitation of copolymer and drug in DMF solutions. All nanoparticles were formed in PBS (0.01 M, pH 7.4) using copolymer concentrations of 0.36 mM. [PTX] solubilized (●), loading efficiency (□). Data points and error bars represent the mean ± SD (n = 3).

All solutions were clear up to a threshold amount of total drug added, after which precipitation was observed upon visual inspection. The amount of drug solubilized increased up to a maximum concentration, above which the solubilized concentration decreased significantly corresponding to the formation of a precipitate. The $MePEG_{114}$-b-PCL_{19} micelles solubilized PTX at a concentration of 40 μg/ml (1.6% w/w) at approximately an 80% loading efficiency, whereas $MePEG_{114}$-b-PCL_{104} nanospheres solubilized the drug at 180 μg/ml (3% w/w) with a 90% loading efficiency. The hydrodynamic diameter of the micelles and nanospheres did not change upon incorporation of PTX and remained at approximately 40 and 80 nm, respectively.

3.3. In vitro paclitaxel release

The *in vitro* release of PTX from nanoparticles at a copolymer concentration of 0.36 mM and a drug loading of 40 μg/ml for both copolymers was investigated (Fig. 5). For both types of nanoparticles, PTX was released in a controlled and sustained fashion with an initial rapid release during the first day followed by a slower release for the remainder of the study. $MePEG_{114}$-b-PCL_{19} micelles released 92% of their drug payload after 7 days, whereas approximately 60% was released from $MePEG_{114}$-b-PCL_{104} nanospheres. Free PTX was released rapidly with complete release of the drug by 12 h.

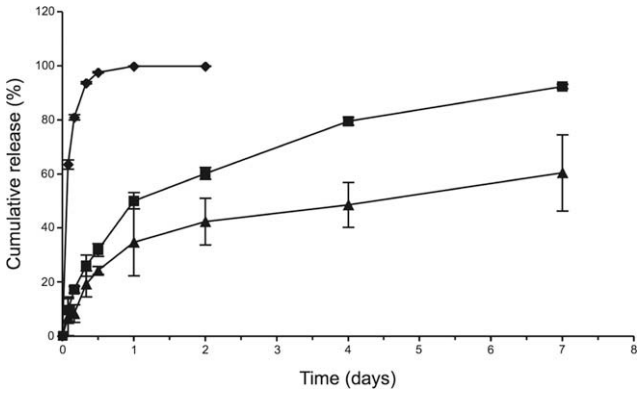

Fig. 5. Release of PTX from dialysis bags. Drug was either in its free form (♦) or solubilized in $MePEG_{114}$-b-PCL_{19} micelles (■) or $MePEG_{114}$-b-PCL_{104} nanospheres (▲) and released into PBS (0.01 M, pH 7.4) at 37 °C. Data points and error bars represent the mean ± SD (n = 3).

3.4. Blood compatibility and plasma distribution

3.4.1. Plasma coagulation

Coagulation of human plasma was assessed in the presence of $MePEG_{114}$-b-PCL_{19} micelles or $MePEG_{114}$-b-PCL_{104} nanospheres with varying copolymer concentrations (Fig. 6). Changes in the extrinsic and common coagulation pathways were evaluated by measurements of the prothrombin time (PT). No statistical difference in PT was found for plasma incubated with either type of nanoparticle as compared to the PBS control. The intrinsic pathway was evaluated using activated partial thromboplastin time (APTT). The APTT was decreased for $MePEG_{114}$-b-PCL_{19} at the highest concentration tested, 0.36 mM, and increased for $MePEG_{114}$-b-PCL_{104} at 0.0036 mM, as compared to the PBS control.

3.4.2. Hemolysis

Neither $MePEG_{114}$-b-PCL_{19} micelles or $MePEG_{114}$-b-PCL_{104} nanospheres induced significant amounts of hemolysis of erythrocytes over a 12-h incubation time at concentrations below 0.1% w/v. The positive control, $MePEG_{17}$-b-PCL_4, induced approximately 30% hemolysis at a concentration of 0.05% w/v. When the polymer concentration was increased to 0.1% w/v there was a small amount of hemolysis (5%) by $MePEG_{114}$-b-PCL_{104} nanospheres at 12 h. However, this level of hemolysis was small compared to the considerable amount of hemolysis (40% at 6 h) that was observed for micellar solutions of $MePEG_{17}$-b-PCL_4 at this concentration (Fig. 7).

3.4.3. PTX plasma distribution

The distribution of PTX in plasma as a function of its formulation was examined. The control groups consisted of PTX loaded micelles, nanospheres or free PTX incubated in distilled water. All fractions of the control groups were clear and colourless with the exception of the samples containing the $MePEG_{114}$-b-PCL_{104} nanospheres. In these samples an opalescent layer was present in the 1.063 g/ml fraction, close to the interface with the 1.21 g/ml fraction. This layer was termed the nanoparticle fraction (“NP fraction”) and its position was marked on the outside of the tube and carefully separated from the remainder of the 1.063 g/ml fraction and analyzed for ^{3}H PTX. Although the “NP fraction” was not visually present in the micellar and free PTX samples, in order to remain consistent, the equivalent layer was removed from these samples and analyzed for ^{3}H PTX. It was found that 100% of the ^{3}H PTX formulated in $MePEG_{114}$-b-PCL_{104} and 76% of the ^{3}H PTX formulated in $MePEG_{114}$-b-PCL_{19} were recovered in the “NP fraction” in distilled water (Fig. 8).

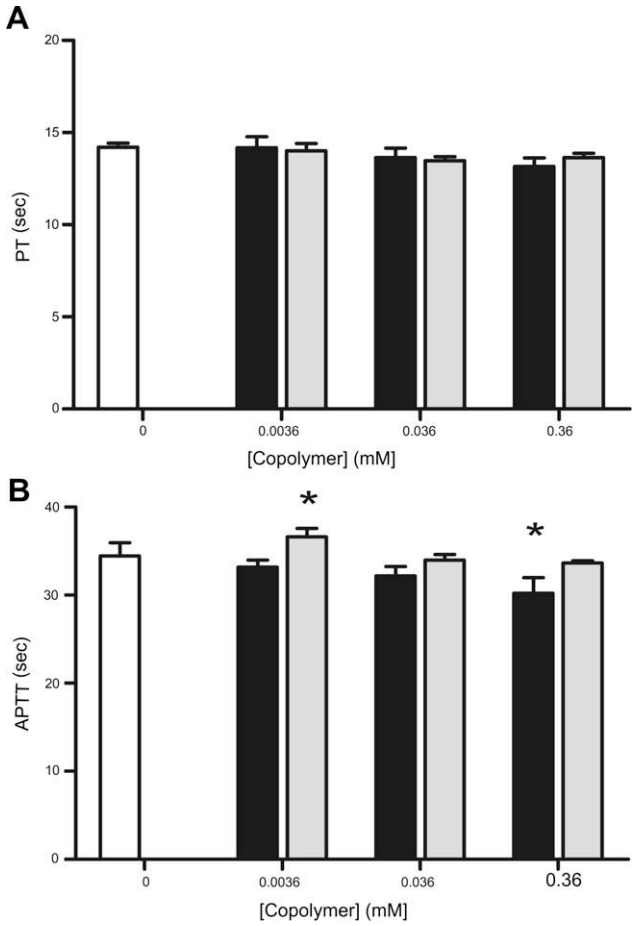

Fig. 6. Effect of nanoparticle type and concentration on the (A) prothrombin time (PT) and (B) activated partial thromboplastin time (APTT). White bars represent control (PBS), black bars represent $MePEG_{114}$-b-PCL_{19} micelles, grey bars represent $MePEG_{114}$-b-PCL_{104} nanospheres. All bars represent mean clotting time ± SD (n = 3). $^*p < 0.05$, different from control.

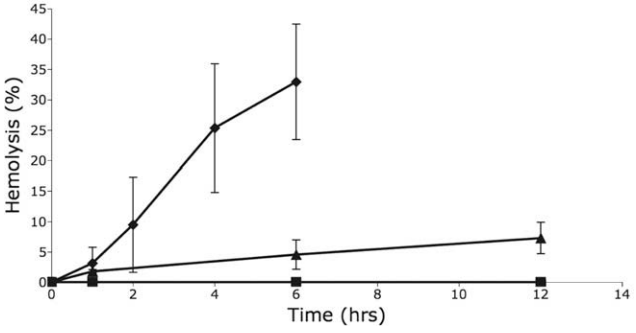

Fig. 7. Time course of hemolysis by $MePEG_{17}$-b-PCL_4 micelles (♦), $MePEG_{114}$-b-PCL_{19} micelles (■), and $MePEG_{114}$-b-PCL_{104} nanospheres (▲) at 37 °C at copolymer concentrations of 0.1% w/v. Data represent mean ± SD (n = 3).

Following density gradient ultracentrifugation of free PTX or micellar PTX incubated in plasma, four visibly distinct layers were observed representing, from top to bottom, the VLDL, LDL, HDL, and LPDP fractions, corresponding to the 1.006, 1.063, 1.21, and 1.25 g/ml density layers, respectively. After centrifugation of the $MePEG_{114}$-b-PCL_{104} samples, again, the thin, opalescent “NP fraction” at the bottom of the 1.063 g/ml (LDL) fraction, close to the interface with 1.21 g/ml (HDL) density layer was observed. This layer was carefully separated and analyzed for ^{3}H PTX content

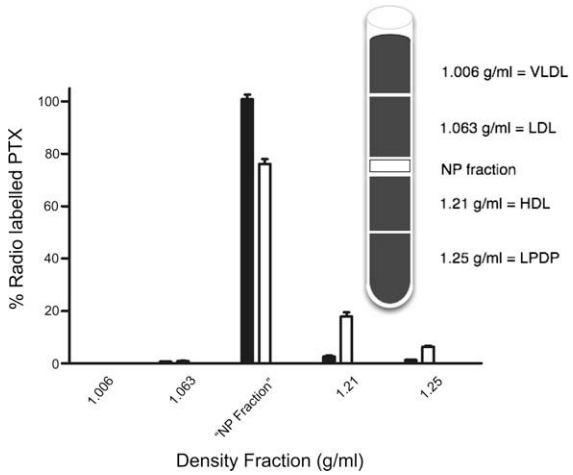

Fig. 8. Partitioning of PTX into various density fractions after a 1-h incubation in distilled water. Drug was formulated in either $MePEG_{114}$-b-PCL_{19} micelles (white) or $MePEG_{114}$-b-PCL_{104} nanospheres (black). All values represent mean ± SD ($n = 6$). Inset is a schematic of an ultracentrifuge tube with the position of the various density fractions and their corresponding lipoprotein fractions after ultracentrifugation. NP fraction represents the clearly separated white band of $MePEG_{114}$-b-PCL_{104} nanospheres.

along with the other layers. Again, to remain consistent, this same fraction was also removed from the plasma samples containing free PTX and $MePEG_{114}$-b-PCL_{19} micelles and termed the "NP fraction", even though this layer was clear in these samples. After incubation of free PTX in human plasma, approximately 50% of the ^{3}H PTX was found in the LPDP fraction and the remaining drug was equally distributed among the other fractions with the exception of the VLDL fraction, which contained very little drug (Fig. 9). The plasma distribution of PTX solubilized in $MePEG_{114}$-b-PCL_{19} micelles was similar to that of free PTX, with approximately 50% of the drug found in the LPDP fraction and an equal distribution of the remaining drug in the other fractions (Fig. 9). For PTX formulated in $MePEG_{114}$-b-PCL_{104} nanospheres, approximately 45% of the radiolabelled drug was found in the "NP fraction" with approximately 35% of the remaining ^{3}H PTX found in the LPDP fraction (Fig. 9). To further investigate this effect, free drug was first incubated in plasma for 10 min followed by the addition of blank $MePEG_{114}$-b-PCL_{104} nanospheres and an additional 1 h incubation. The ^{3}H PTX distribution was similar to the data for the previous experiment in which most of the ^{3}H PTX was found in the "NP fraction" and the majority of the remaining drug in the LPDP fraction (Fig. 9). There were some statistically significant changes in the distribution of free and nanoparticulate PTX over the incubation times. In the absence of any clear trend in the data, these differences were not given further consideration.

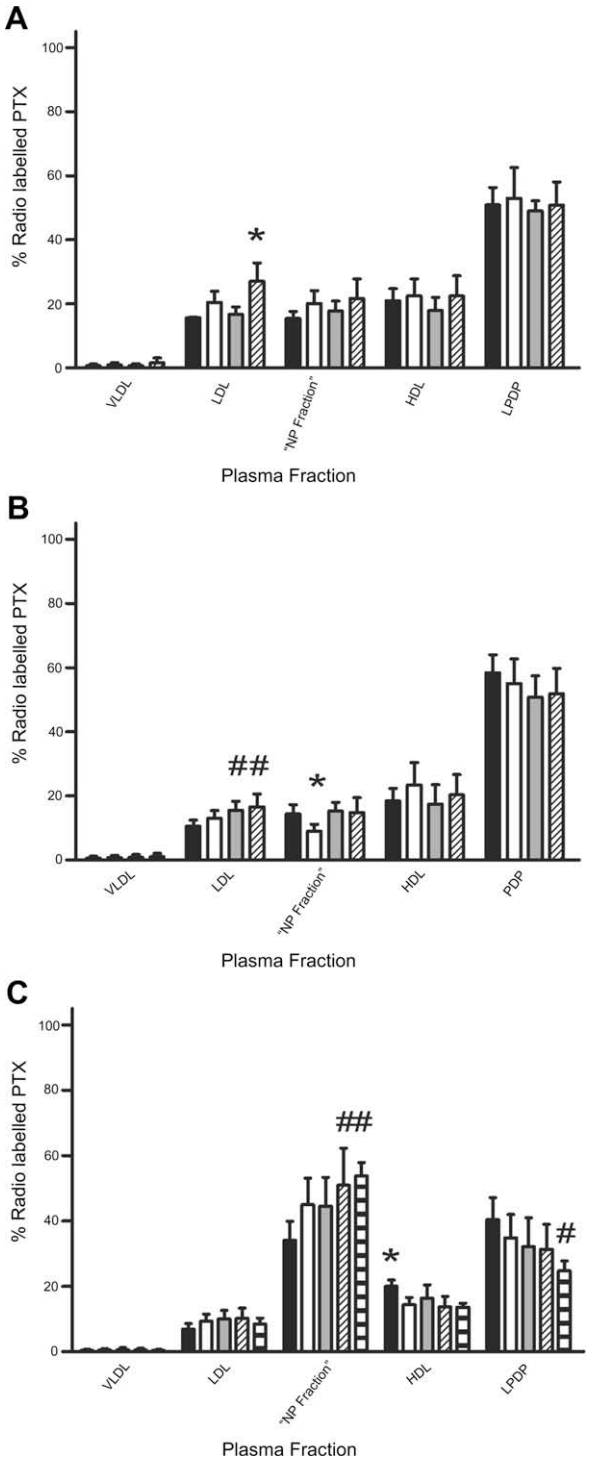

Fig. 9. Time dependence of partitioning of (A) free PTX, (B) $MePEG_{114}$-b-PCL_{19} micellar PTX (C) $MePEG_{114}$-b-PCL_{104} nanosphere PTX into various human plasma fractions during incubation times of 1 h (black), 6 h (white), 12 h (grey), and 24 h (diagonal stripes). Horizontal striped bars in (C) represent distribution of PTX after incubation of free PTX for 10 min followed by addition of blank $MePEG_{114}$-b-PCL_{104} nanospheres and an additional 1 h incubation. All values represent mean ± SD ($n = 6$). $^*p < 0.05$, different from all other samples in plasma fraction. $^\#p < 0.05$, different from 1 h sample in plasma fraction.

4. Discussion

The terminal hydroxyl group of MePEG was used as the initiator for the ring opening polymerization of caprolactone to synthesize two MePEG-b-PCL diblock copolymers, both with a MePEG molecular weight of 5000 g/mol, but two very different PCL block lengths. As previously described by our group, the copolymer composition resulting from this reaction could be controlled in a predictable way by variation of the feed ratio of the reactants in the starting mixture [35,40]. As determined by ^{1}H NMR, the degree of polymerization of the two copolymers was $MePEG_{114}$-b-PCL_{19} and $MePEG_{114}$-b-PCL_{104}, which matched very closely to the theoretical values (Table 1). The experimental molecular weights as determined by GPC deviated from the theoretical values more so for $MePEG_{114}$-b-PCL_{104}, most likely due to the fact that the PEG standards are structurally dissimilar to this copolymer, which is composed of a large fraction of PCL.

Table 1
Characterization data of synthesized MePEG-b-PCL copolymers

Feed ratio[a]	DPn[b]	MW Theo[c] (g/mol)	MW NMR[d] (g/mol)	MW GPC[e] (g/mol)	PDI[f]	Diameter[g] (nm)
70:30	$MePEG_{114}$-b-PCL_{19}	7143	7166	7044	1.18	39.2 ± 1.3
30:70	$MePEG_{114}$-b-PCL_{104}	16,651	16,856	12,238	1.47	81.4 ± 1.0

[a] Feed weight ratio of MePEG:caprolactone.
[b] Degree of polymerization of MePEG:MW_{MePEG}/44, DPn of PCL: rounded off value determined by NMR.
[c] Theoretical MW based on feed weight ratio.
[d] MW determined by NMR.
[e] MW determined by GPC.
[f] Polydispersity index determined by GPC.
[g] Nanoparticle hydrodynamic diameter determined by PCS based on scattering intensity at 37 °C at a [copolymer] of 0.36 mM. Diameters did not change upon loading of PTX.

Nanoparticles were formed by the solvent displacement method also referred to as nanoprecipitation. This method was chosen due to the low aqueous solubility of the $MePEG_{114}$-b-PCL_{104} copolymer requiring that the copolymer first be dissolved in an organic solvent. Although $MePEG_{114}$-b-PCL_{19} was readily water soluble, which allows for the formation of micelles by direct dissolution, to ensure consistent preparation methods for both copolymers, $MePEG_{114}$-b-PCL_{19} micelles were formed by nanoprecipitation. The hydrodynamic diameters of the formed nanoparticles at a concentration of 0.36 mM, as determined by DLS, were found to be dependent on the length of the hydrophobic block. Nanospheres composed of $MePEG_{114}$-b-PCL_{104} had a diameter of 80 nm, approximately twice as large as the $MePEG_{114}$-b-PCL_{19} micelles. Electron micrographs revealed that the nanoparticles had a spherical morphology; however, the diameters of the nanoparticles did not agree with the light scattering results. Visually, the nanoparticles appeared to be significantly smaller, particularly for the $MePEG_{114}$-b-PCL_{19} micelles. This observation has been described by other research groups and was rationalized by the fact that only the dense core of the nanoparticles is evident in the micrographs [41]. Since the core block of the $MePEG_{114}$-b-PCL_{19} micelles is relatively short, it is to be expected that the diameter of the micelles in the TEM image is considerably smaller than that determined by DLS. Interestingly, the hydrodynamic diameter of the nanospheres formed from $MePEG_{114}$-b-PCL_{104} had a clear dependence on the concentration of copolymer used in their formation. Riley et al. also observed a concentration dependence on the hydrodynamic diameter of MePEG-b-PDLLA nanoparticles with long PDLLA blocks [42]. In these studies, a series of MePEG-b-PDLLA copolymers with a fixed MePEG block length and increasing PDLLA molecular weights were synthesized. It was observed that the nanoparticles formed by copolymers with relatively low PDLLA molecular weights had hydrodynamic radii dependent only on the hydrophobic block length, and this radius scaled linearly with the number of hydrophobic blocks, characteristic of block copolymer micelles. Conversely, once the hydrophobic block reached a critical length; the hydrodynamic radii of the nanoparticles became highly dependent on the concentration of copolymer used in the organic phase prior to nanoprecipitation, similar to nanoparticles formed from homopolymers [42]. In this study, the scaling relationship between hydrophobic block length and hydrodynamic radii could not be explored, since only two hydrophobic block lengths were investigated. However, the size dependence on copolymer concentration for $MePEG_{114}$-b-PCL_{104} suggests that a critical hydrophobic block length had been reached, beyond which, micelles are no longer formed, similar to the findings of Riley et al. [42].

Using fluorescence anisotropy, we showed that as the PCL block length increased there was a significant increase in the microviscosity of the nanoparticle cores. It has been documented that the fluorescence probe DPH partitions into the hydrophobic domain of membranes and core region of micelles [40,43]. This probe is sensitive to the microviscosity of its surroundings and displays changes in its depolarization as measured by fluorescence anisotropy. A smaller anisotropy value indicates a lower degree of depolarization and therefore, a less viscous environment. As a positive control, DPH was solubilized in a sphingomyelin bilayer. Upon heating the sphingomyelin, the anisotropy value dropped significantly between 33 and 47 °C, with a midpoint at approximately 40 °C, characteristic of the phase transition of the bilayer from a gel to a less viscous liquid crystalline state [44]. Both copolymer nanoparticles displayed a slight decrease in the anisotropy, implying a decrease in the microviscosity of the core during heating. However, $MePEG_{114}$-b-PCL_{104} nanospheres were considerably more viscous than $MePEG_{114}$-b-PCL_{19} micelles over the whole temperature range. As a comparison, DPH was solubilized in polysorbate 20 micelles. Anisotropy values for $MePEG_{114}$-b-PCL_{19} were considerably higher than those of the short chain surfactant micelles of polysorbate 20, indicating a higher viscosity core, presumably due to the longer, entangled chains of the PCL. Similar to our findings, Lavasanifar et al. used the hydrophobic, fluorescent probe 1,3-(1,1′-dipyrenyl)propane to show that increased poly(L-amino acid) (PLAA) block lengths induced a noticeable increase in the core microviscosity of MePEG-b-PLAA micelles [45]. Studies by Heald et al. used ^{1}H NMR techniques to show that as the PDLLA block of MePEG-b-PDLLA copolymers increased, the hydrophobic core became more solid like [32]. Thus, our findings confirm those of other researchers, suggesting that the microviscosity of the hydrophobic core is correlated to the length of the core-forming blocks. The short hydrophobic block, water-soluble $MePEG_{114}$-b-PCL_{19} copolymer, formed micelles with a relatively low viscosity core. Conversely, the more hydrophobic $MePEG_{114}$-b-PCL_{104} copolymer formed nanospheres with a more solid-like core, characterized by a higher microviscosity.

The PTX solubilization capacity of nanoparticulate dispersions of each of the synthesized copolymers was investigated. For each solution, the amount of drug solubilized increased up to a maximum concentration, above which drug precipitation occurred with a corresponding decrease in the solubilized drug concentration and loading efficiency (Fig. 4). The $MePEG_{114}$-b-PCL_{104} nanosphere formulation solubilized more drug at a higher loading efficiency than that of the $MePEG_{114}$-b-PCL_{19} micelles, which may be attributed to the larger core volume of $MePEG_{114}$-b-PCL_{104} nanospheres as indicated by the cryo TEM micrographs and hydrodynamic diameters. A review of the literature indicates that the amount of PTX solubilized by diblock copolymers can range from 0.5% up to 25% w/w [3,46]. A number of factors may be responsible for the variable PTX loadings among groups, including differences in hydrophobic block length and preparation method. The compatibility between the drug and core-forming block has also been shown to be a contributing factor in the amount of drug that can be solubilized by nanoparticles. Lui et al. demonstrated that the hydrophobic anticancer compound, ellipticine, was solubilized by MePEG-b-PCL to

a greater extent than by MePEG-b-PDLLA [47]. This group attributed the difference to a greater degree of compatibility between PCL and the drug, as calculated by solubility parameters and the enthalpy of mixing. Recently, our group demonstrated that the amount of drug solubilized by MePEG-b-PCL micelles was directly correlated to the compatibility between the hydrophobic block and drug, as determined by the calculated Flory Huggins interaction parameter [34]. Furthermore, our compatibility calculations predicted that PTX is not highly compatible with PCL, which was demonstrated experimentally by a low solubilization of PTX. Zhang et al. were able to achieve PTX loading levels of 25% w/w in MePEG-b-PDLLA micelles using the film hydration method [3]. In this study, we were not able to attain as high of a drug loading, likely due a lower compatibility between PTX and PCL as compared to PTX and PDLLA. In addition, the method of preparation can affect drug loading. In our previous studies, we were able to solubilize more PTX in MePEG-b-PCL micelles using a film hydration method [34]. However, film hydration of water insoluble copolymers is not possible, therefore, for this study, dialysis was necessary to produce nanospheres from the $MePEG_{114}$-b-PCL_{104} copolymer.

Free PTX was released from the dialysis bags at a rapid rate with complete depletion of the drug from the bags by 12 h, thus demonstrating that the dialysis membrane would not retard the release of the drug from nanoparticles to any great extent. Paclitaxel was released from both formulations in a controlled and sustained manner for greater than 7 days. A 7-day release study was chosen as pharmacokinetic studies of drug loaded nanoparticles have demonstrated that the blood circulation time for nanoparticulate systems rarely exceeds 2 days [14,26,48]. Seven days were sufficiently long enough to see differences in the drug release profiles of micelles and nanospheres, providing evidence that PTX is retained longer when encapsulated in nanospheres. During the first day of drug release, nanospheres and micelles had similar release profiles, which may be explained by rapid PTX release from the core and shell interface. After the first day, the release rates from both nanoparticles slowed, indicative of drug release from the core. The release of PTX was faster from $MePEG_{114}$-b-PCL_{19} micelles, with nearly all the drug (92%) released by 7 days. The $MePEG_{114}$-b-PCL_{104} nanospheres released approximately 60% of loaded drug in 7 days. Other groups have also found that an increase in the hydrophobic block decreases the release rate of the encapsulated drug. Deng and coworkers found that an increase in the molecular weight of the PLLA block of MePEG-PLLA diblock copolymers from 3515 to 4247 g/mol resulted in a decrease in the cumulative PTX release of almost 10% over 4 days [49]. Likewise, Kim et al. showed that increases in the PCL block length decreased the release rate of indomethacin [50]. In both of these cases, the decrease in the release rate was attributed to the increased interaction between the longer hydrophobic block of the nanoparticles and the drug. The higher microviscosity and larger diameter of the hydrophobic core of the nanospheres may also be attributed to a slower drug release rate, as these factors will decrease the diffusion rate of the drug through the PCL [51]. Similar to the *in vitro* release of other hydrophobic drugs such as indomethacin, ellipticine and rapamycin, from MePEG-b-PCL nanoparticles, 100% drug release was not achieved by 7 days [50–52]. It is assumed that the remaining drug was still associated with the PCL core.

It is evident that a systemically administered drug carrier system must be hemocompatible. For a range of concentrations, the two copolymers were tested for compatibility with human blood by investigating their ability to alter coagulation times and cause hemolysis. The effects on coagulation were evaluated by analyzing the activated partial thromboplastin time (APTT) and the prothrombin time (PT). The APTT was found to be significantly decreased for micelles at the highest concentration and increased at the lowest nanospheres concentration as compared to the PBS control. However, these differences were considered to be of minor concern as the experimental values were well within the normal range of coagulation times of 32–46 s for APTT [53]. The lack of activation of the coagulation system may be attributed to the highly hydrated PEG brush-like covering of the surfaces of nanoparticles. PEGylated nanoparticle surfaces have been shown to inhibit the adsorption of various plasma proteins, including plasma factors of the coagulation system, thus, preventing the activation of the coagulation cascade [7,8].

Of critical importance for systemically administered amphiphilic copolymer systems is their hemolytic potential. It is well known that surfactants at high enough concentrations are capable of disrupting cell membranes, such as those of erythrocytes, by penetration and saturation of the membrane with unimers followed by solubilization of the membrane lipids and proteins [54,55]. As shown previously by our group, the short block length copolymer $MePEG_{17}$-b-PCL_4 was capable of inducing rapid and significant hemolysis [38]. In this study, there was no significant hemolysis when erythrocytes were incubated with either the $MePEG_{114}$-b-PCL_{19} micelles or $MePEG_{114}$-b-PCL_{104} nanospheres. Our previous work has shown that $MePEG_{114}$-b-PCL_{19} has a relatively low critical micelle concentration of 6.29×10^{-7} M, indicating a low number of unimers in solution and a high degree of thermodynamic stability [34]. We suggest that the stable core and well-hydrated corona of these nanoparticles would result in intact nanoparticles with few available unimers available for penetration into the cell membrane, thus, reducing membrane perturbation and subsequent hemolysis.

Free paclitaxel is highly bound to plasma proteins, specifically albumin and alpha-1-acid glycoprotein [56]. In this study, the incubation of free PTX led to the partitioning of the drug equally into the LPDP (i.e. primarily albumin and alpha-1-acid glycoprotein) and lipoprotein fractions. The distribution of the free drug did not change over the incubation times tested, indicating the rapid distribution of PTX among the plasma components and confirming our earlier findings [24]. When PTX encapsulated in $MePEG_{114}$-b-PCL_{19} micelles was incubated in distilled water and separated by density gradient centrifugation, the majority of PTX was found in the lower portion of the 1.063 g/ml density fraction, or what we termed the NP fraction (Fig. 8). We believe that the PTX found in this density fraction primarily remained associated with the micelles since the final concentration of copolymer after incubation, layering and centrifugation was still well above the CMC previously determined for this copolymer [34]. Incubation of the micelles in plasma dramatically changed the distribution of the drug so that 50% of the drug was associated with the LPDP fraction, similar to that of free PTX. Since the copolymer concentration was maintained well above the CMC, we believe this effect was not caused by destabilization of the micelles due to dilution, but rather from an interaction with plasma components. A similar drug distribution was found previously when PTX was solubilized by MePEG-b-PDLLA micelles [24]. These findings suggest a few possibilities. Upon incubation in plasma, it is possible that there was disruption of the micellar structure and/or rapid drug release and partitioning into the LPDP and lipoprotein fractions. The other possibility is that the intact micelles with their drug payload were associated with the plasma fractions. Due to the fact that we were not able to assay the copolymer in the various plasma fractions, it was not possible to determine whether the drug was still associated with the copolymer. Previously, our group investigated the biodistribution of ^{3}H PTX solubilized in ^{14}C MePEG-b-PDLLA micelles in male Sprague–Dawley rats [22]. It was found that PTX rapidly dissociated from the micellar components, and the copolymer accumulated in the kidneys and bladder resulting in copolymer elimination through the urine. Conversely, the PTX was widely distributed

among the tissues, and the majority of the drug was eliminated in the feces. These results provide strong evidence for the possibility of rapid release of the micellar drug during incubation in plasma, resulting in similar plasma profiles for free and micellar PTX. The rapid partitioning of PTX from the micelles into the LPDP was not reflected by the relatively slow *in vitro* release rate of micellar PTX. A release study using plasma as the release media, or PBS containing plasma proteins, may have more accurately predicted the micelle instability in plasma. However, in order to do so, a dialysis membrane with a large molecular weight cut off would need to be used in order to enable proteins to freely equilibrate between the micellar solution and the release media [57]. This method has limitations, as it is likely that micelles and/or unimers may be released from the dialysis membrane and removed by maintenance of sink conditions, resulting in either rapid release of the drug or dilution below the CMC.

When PTX encapsulated in $MePEG_{114}$-b-PCL_{104} nanospheres was incubated in distilled water, it was possible to visualize and separate out the nanospheres from the other density fractions since the nanospheres centrifuged into a separate, concentrated layer (NP fraction) located between the 1.063 and 1.21 g/ml density fractions. It was found that 100% of the encapsulated ^{3}H PTX was recovered from this fraction, demonstrating that the encapsulated drug remained associated with the $MePEG_{114}$-b-PCL_{104} copolymer during the ultracentrifugation process. Upon incubation in plasma, again the nanospheres were found in the same density fraction as when they were incubated in distilled water. The largest amount of the ^{3}H PTX was found in this layer with the majority of the remaining drug in the LPDP fraction. Since the nanoparticles were separated due to their density and this separation did not change when incubated in plasma, it was not possible to establish whether the nanospheres were associated with lipoproteins in the plasma prior to ultracentrifugation. However, the key finding is that the $MePEG_{114}$-b-PCL_{104} nanospheres retained more of their drug payload, releasing less of it to the LPDP fraction, compared to $MePEG_{114}$-b-PCL_{19} micelles or free drug. The increased drug retention by the nanospheres in the presence of plasma proteins may be attributed to the larger, more viscous, solid-like core of the nanospheres. Interestingly, when free PTX was incubated in plasma, followed by the addition of blank $MePEG_{114}$-b-PCL_{104} nanospheres, again the majority of the drug was found in the NP fraction, indicating association of PTX with the nanospheres, possibly at the interface between the PCL and MePEG blocks.

5. Conclusions

In this study we have shown that increasing the hydrophobic block length of MePEG-b-PCL copolymers results in a dramatic shift in the physicochemical properties of nanoparticles made from this polymer. The readily water-soluble $MePEG_{114}$-b-PCL_{19} formed micellar structure particles with a small average hydrodynamic diameter that did not vary with copolymer concentration and possessed a low core microviscosity. The water insoluble $MePEG_{114}$-b-PCL_{104} formed nanospheres characterized by a larger hydrodynamic diameter that increased with copolymer concentration and a more solid-like core. Compared to the micelles, nanospheres solubilized more PTX and released it at slower rates. There was no major difference in the hemocompatibility between the two types of nanoparticles as determined by coagulation times and hemolysis. When PTX loaded micelles and nanospheres were incubated in human plasma, the majority of the micellar drug was associated with the lipoprotein deficient plasma fraction (LPDP), similar to the plasma distribution profile of free PTX. On the other hand, the majority of PTX solubilized in nanospheres was found associated with these nanoparticles in a distinct density fraction, well separated from the LPDP fraction. These results demonstrate that the nanospheres have a high affinity for PTX allowing them to retain their drug payload when incubated in human plasma as compared to micelles. Studies are underway to examine the pharmacokinetic profiles of PTX loaded nanospheres and micelles.

Acknowledgements

These studies were financially funded by grants from the Canadian Institutes of Health Research (CIHR) and the Natural Sciences and Engineering Research Council awarded to Helen Burt and by a CIHR Clinical Research Initiative Doctoral Research Award provided to Kevin Letchford.

References

[1] M. Yokoyama, T. Okano, Y. Sakurai, H. Ekimoto, C. Shibazaki, K. Kataoka, Toxicity and antitumor activity against solid tumors of micelle-forming polymeric anticancer drug and its extremely long circulation in blood, Cancer Res. 51 (12) (1991) 3229–3236.
[2] A.V. Kabanov, E.V. Batrakova, N.S. Melik-Nubarov, N.A. Fedoseev, T.Y. Dorodnich, V.Y. Alakhov, V.P. Chekhonin, I.R. Nazarova, V.A. Kabanov, A new class of drug carriers: micelles of poly(oxyethylene)–poly(oxypropylene) block copolymers as microcontainers for drug targeting from blood in brain, J. Control. Release 22 (2) (1992) 141–157.
[3] X. Zhang, J.K. Jackson, H.M. Burt, Development of amphiphilic diblock copolymers as micellar carriers of taxol, Int. J. Pharm. 132 (1,2) (1996) 195–206.
[4] C. Allen, J. Han, Y. Yu, D. Maysinger, A. Eisenberg, Polycaprolactone-b-poly(ethylene oxide) copolymer micelles as a delivery vehicle for dihydrotestosterone, J. Control. Release 63 (3) (2000) 275–286.
[5] H.S. Yoo, T.G. Park, Biodegradable polymeric micelles composed of doxorubicin conjugated PLGA-PEG block copolymer, J. Control. Release 70 (1–2) (2001) 63–70.
[6] D. Bazile, C. Prud'Homme, M.T. Bassoullet, M. Marland, G. Spenlehauer, M. Veillard, Stealth MePEG-PLA nanoparticles avoid uptake by the mononuclear phagocytes system, J. Pharm. Sci. 84 (4) (1995) 493–498.
[7] R. Gref, M. Luck, P. Quellec, M. Marchand, E. Dellacherie, S. Harnisch, T. Blunk, R.H. Muller, 'Stealth' corona-core nanoparticles surface modified by polyethylene glycol (PEG): influences of the corona (PEG chain length and surface density) and of the core composition on phagocytic uptake and plasma protein adsorption, Colloids Surf. B 18 (3,4) (2000) 301–313.
[8] H. Sahli, J. Tapon-Bretaudiere, A.-M. Fischer, C. Sternberg, G. Spenlehauer, T. Verrecchia, D. Labarre, Interactions of poly(lactic acid) and poly(lactic acid-co-ethylene oxide) nanoparticles with the plasma factors of the coagulation system, Biomaterials 18 (4) (1997) 281–288.
[9] K. Letchford, H. Burt, A review of the formation and classification of amphiphilic block copolymer nanoparticulate structures: micelles, nanospheres, nanocapsules and polymersomes, Eur. J. Pharm. Biopharm. 65 (3) (2007) 259–269.
[10] P. Alexandridis, A.T. Hatton, Poly(ethylene oxide)–poly(propylene oxide)–poly(ethylene oxide) block copolymer surfactants in aqueous solutions and at interfaces: thermodynamics, structure, dynamics, and modeling, Colloids Surf. A 96 (1/2) (1995) 1–46.
[11] A.N. Martin, Chapter 15: Colloids, in: A.N. Martin (Ed.), Physical Pharmacy: Physical Chemical Principles in the Pharmaceutical Sciences, Williams and Wilkins, Baltimore, 1993, pp. 393–422.
[12] R. Gref, Y. Minamitake, M.T. Peracchia, V. Trubetskoy, V. Torchilin, R. Langer, Biodegradable long-circulating polymer nanospheres, Science 263 (5153) (1994) 1600–1603.
[13] G.S. Kwon, M. Yokoyama, T. Okano, Y. Sakurai, K. Kataoka, Biodistribution of micelle-forming polymer–drug conjugates, Pharm. Res. 10 (7) (1993) 970–974.
[14] G. Kwon, S. Suwa, M. Yokoyama, T. Okano, Y. Sakurai, K. Kataoka, Enhanced tumor accumulation and prolonged circulation times of micelle-forming poly(ethylene oxide-aspartate) block copolymer–adriamycin conjugates, J. Control. Release 29 (1–2) (1994) 17–23.
[15] V. Alakhov, E. Klinski, S. Li, G. Pietrzynski, A. Venne, E. Batrakova, T. Bronitch, A. Kabanov, Block copolymer-based formulation of doxorubicin. From cell screen to clinical trials, Colloids Surf. B 16 (1–4) (1999) 113–134.
[16] R.T. Dorr, Pharmacology and toxicology of Cremophor EL diluent, Ann. Pharmacother. 28 (5 Suppl.) (1994) S11–S14.
[17] X. Zhang, H.M. Burt, G. Mangold, D. Dexter, D. Von Hoff, L. Mayer, W.L. Hunter, Anti-tumor efficacy and biodistribution of intravenous polymeric micellar paclitaxel, Anticancer Drugs 8 (7) (1997) 696–701.
[18] S.C. Kim, D.W. Kim, Y.H. Shim, J.S. Bang, H.S. Oh, S.W. Kim, M.H. Seo, In vivo evaluation of polymeric micellar paclitaxel formulation: toxicity and efficacy, J. Control. Release 72 (1–3) (2001) 191–202.
[19] F. Ahmed, R.I. Pakunlu, A. Brannan, F. Bates, T. Minko, D.E. Discher, Biodegradable polymersomes loaded with both paclitaxel and doxorubicin permeate and shrink tumors, inducing apoptosis in proportion to accumulated drug, J. Control. Release 116 (2) (2006) 150–158.

[20] L.-m. Han, J. Guo, L.-j. Zhang, Q.-s. Wang, X.-l. Fang, Pharmacokinetics and biodistribution of polymeric micelles of paclitaxel with pluronic P123, Acta Pharmacol. Sin. 27 (6) (2006) 747–753.
[21] T. Hamaguchi, Y. Matsumura, M. Suzuki, K. Shimizu, R. Goda, I. Nakamura, I. Nakatomi, M. Yokoyama, K. Kataoka, T. Kakizoe, NK105, a paclitaxel-incorporating micellar nanoparticle formulation, can extend in vivo antitumour activity and reduce the neurotoxicity of paclitaxel, Br. J. Cancer 92 (7) (2005) 1240–1246.
[22] H.M. Burt, X. Zhang, P. Toleikis, L. Embree, W.L. Hunter, Development of copolymers of poly(DL-lactide) and methoxypolyethylene glycol as micellar carriers of paclitaxel, Colloids Surf. B 16 (1–4) (1999) 161–171.
[23] D. Le Garrec, S. Gori, L. Luo, D. Lessard, D.C. Smith, M.A. Yessine, M. Ranger, J.C. Leroux, Poly(*N*-vinylpyrrolidone)-block-poly(DL-lactide) as a new polymeric solubilizer for hydrophobic anticancer drugs: in vitro and in vivo evaluation, J. Control. Release 99 (1) (2004) 83–101.
[24] M. Ramaswamy, X. Zhang, H.M. Burt, K.M. Wasan, Human plasma distribution of free paclitaxel and paclitaxel associated with diblock copolymers, J. Pharm. Sci. 86 (4) (1997) 460–464.
[25] J. Liu, F. Zeng, C. Allen, In vivo fate of unimers and micelles of a poly(ethylene glycol)-block-poly(caprolactone) copolymer in mice following intravenous administration, Eur. J. Pharm. Biopharm. 65 (3) (2007) 309–319.
[26] N.Y. Yamamoto, Y. Kato, Y. Sugiyama, K. Kataoka, Long-circulating poly(ethylene glycol)-poly(D,L-lactide) block copolymer micelles with modulated surface charge, J. Control. Release 77 (2001) 27–38.
[27] J.H. Kim, K. Emoto, M. Ijima, Y. Nagasaki, T. Aoyagi, T. Okano, Y. Sakurai, K. Kataoka, Core-stabilized polymeric micelle as potential drug carrier: increased solubilization of taxol, Polym. Adv. Tech. 10 (1999) 647–654.
[28] X. Shuai, T. Merdan, A.K. Schaper, F. Xi, T. Kissel, Core-cross-linked polymeric micelles as paclitaxel carriers, Bioconjug. Chem. 15 (3) (2004) 441–448.
[29] X. Zhang, Y. Li, X. Chen, X. Wang, X. Xu, Q. Liang, J. Hu, X. Jing, Synthesis and characterization of the paclitaxel/MPEG-PLA block copolymer conjugate, Biomaterials 26 (14) (2005) 2121–2128.
[30] M.L. Forrest, J.A. Yanez, C.M. Remsberg, Y. Ohgami, G.S. Kwon, N.M. Davies, Paclitaxel prodrugs with sustained release and high solubility in poly(ethylene glycol)-b-poly(e-caprolactone) micelle nanocarriers: pharmacokinetic disposition, tolerability, and cytotoxicity, Pharm. Res. 25 (1) (2008) 194–206.
[31] C. Allen, D. Maysinger, A. Eisenberg, Nano-engineering block copolymer aggregates for drug delivery, Colloids Surf. B 16 (1999) 3–27.
[32] C.R. Heald, S. Stolnik, K.S. Kujawinski, C. De Matteis, M.C. Garnett, L. Illum, S.S. Davis, S.C. Purkiss, R.J. Barlow, P.R. Gellert, Poly(lactic acid)–poly(ethylene oxide) (PLA-PEG) nanoparticles: NMR studies of the central solid-like PLA core and the liquid PEG corona, Langmuir 18 (9) (2002) 3669–3675.
[33] G.S. Kwon, Diblock copolymer nanoparticles for drug delivery, Crit. Rev. Ther. Drug Carrier Syst. 15 (5) (1998) 481–512.
[34] K. Letchford, R. Liggins, H. Burt, Solubilization of hydrophobic drugs by methoxy poly(ethylene glycol)-block-polycaprolactone diblock copolymer micelles: theoretical and experimental data and correlations, J. Pharm. Sci. 97 (3) (2008) 1179–1190.
[35] K. Letchford, J. Zastre, R. Liggins, H. Burt, Synthesis and micellar characterization of short block length methoxy poly(ethylene glycol)-block-poly(caprolactone) diblock copolymers, Colloids Surf. B 35 (2) (2004) 81–91.
[36] J. Zastre, J. Jackson, H. Burt, Evidence for modulation of P-glycoprotein-mediated efflux by methoxypolyethylene glycol-block-polycaprolactone amphiphilic diblock copolymers, Pharm. Res. 21 (8) (2004) 1489–1497.
[37] R.T. Liggins, S. D'Amours, J.S. Demetrick, L.S. Machan, H.M. Burt, Paclitaxel loaded poly(L-lactic acid) microspheres for the prevention of intraperitoneal carcinomatosis after a surgical repair and tumor cell spill, Biomaterials 21 (19) (2000) 1959–1969.
[38] J. Zastre, J.K. Jackson, W. Wong, H.M. Burt, Methoxypolyethylene glycol-block-polycaprolactone diblock copolymers reduce P-glycoprotein efflux in the absence of a membrane fluidization effect while stimulating P-glycoprotein ATPase activity, J. Pharm. Sci. 96 (4) (2007) 864–875.
[39] S.M. Cassidy, F.W. Strobel, K.M. Wasan, Plasma lipoprotein distribution of liposomal nystatin is influenced by protein content of high-density lipoproteins, Antimicrob. Agents Chemother. 42 (8) (1998) 1878–1888.
[40] J. Zastre, J. Jackson, M. Bajwa, R. Liggins, F. Iqbal, H. Burt, Enhanced cellular accumulation of a P-glycoprotein substrate, rhodamine-123, by caco-2 cells using low molecular weight methoxypolyethylene glycol-block-polycaprolactone diblock copolymers, Eur. J. Pharm. Biopharm. 54 (3) (2002) 299–309.
[41] M. Hans, K. Shimoni, D. Danino, S.J. Siegel, A. Lowman, Synthesis and characterization of mPEG-PLA prodrug micelles, Biomacromolecules 6 (5) (2005) 2708–2717.
[42] T. Riley, S. Stolnik, C.R. Heald, C.D. Xiong, M.C. Garnett, L. Illum, S.S. Davis, S.C. Purkiss, R.J. Barlow, P.R. Gellert, Physicochemical evaluation of nanoparticles assembled from poly(lactic acid)–poly(ethylene glycol) (PLA-PEG) block copolymers as drug delivery vehicles, Langmuir 17 (11) (2001) 3168–3174.
[43] X. Zhang, J.K. Jackson, H.M. Burt, Determination of surfactant critical micelle concentration by a novel fluorescence depolarization technique, J. Biochem. Biophys. Methods 31 (3,4) (1996) 145–150.
[44] M. Kuikka, B. Ramstedt, H. Ohvo-Rekila, J. Tuuf, J.P. Slotte, Membrane properties of D-erythro-*N*-acyl sphingomyelins and their corresponding dihydro species, Biophys. J. 80 (5) (2001) 2327–2337.
[45] A. Lavasanifar, J. Samuel, G.S. Kwon, The effect of alkyl core structure on micellar properties of poly(ethylene oxide)-block-poly(L-aspartamide) derivatives, Colloids Surf. B 22 (2) (2001) 115–126.
[46] S.C. Lee, C. Kim, I.C. Kwon, H. Chung, S.Y. Jeong, Polymeric micelles of poly(2-ethyl-2-oxazoline)-block-poly(e-caprolactone) copolymer as a carrier for paclitaxel, J. Control. Release 89 (3) (2003) 437–446.
[47] J. Liu, Y. Xiao, C. Allen, Polymer–drug compatibility: a guide to the development of delivery systems for the anticancer agent ellipticine, J. Pharm. Sci. 93 (1) (2004) 132–143.
[48] H. Montazeri Aliabadi, D.R. Brocks, A. Lavasanifar, Polymeric micelles for the solubilization and delivery of cyclosporine A: pharmacokinetics and biodistribution, Biomaterials 26 (35) (2005) 7251–7259.
[49] L. Deng, A. Li, C. Yao, D. Sun, A. Dong, Methoxy poly(ethylene glycol)-b-poly(L-lactic acid) copolymer nanoparticles as delivery vehicles for paclitaxel, J. Appl. Polym. Sci. 98 (5) (2005) 2116–2122.
[50] S.Y. Kim, I.G. Shin, Y.M. Lee, C.S. Cho, Y.K. Sung, Methoxy poly(ethylene glycol) and epsilon-caprolactone amphiphilic block copolymeric micelle containing indomethacin. II. Micelle formation and drug release behaviours, J. Control. Release 51 (1) (1998) 13–22.
[51] M.L. Forrest, C.-Y. Won, A.W. Malick, G.S. Kwon, In vitro release of the mTOR inhibitor rapamycin from poly(ethylene glycol)-b-poly(e-caprolactone) micelles, J. Control. Release 110 (2) (2006) 370–377.
[52] J. Liu, F. Zeng, C. Allen, Influence of serum protein on polycarbonate-based copolymer micelles as a delivery system for a hydrophobic anti-cancer agent, J. Control. Release 103 (2) (2005) 481–497.
[53] S.L. Perkins, Appendix A: Normal Blood and Bone Marrow Values in Humans, in: J.P. Greer, J. Foerster, J.N. Lukens, G.M. Rodgers, F. Paraskevas, B. Glader (Eds.), Wintrobe's Clinical Hematology, Lippincott Williams and Wilkins, Philadelphia, 2004, p. 2706.
[54] M.N. Jones, Surfactants in membrane solubilisation, Int. J. Pharm. 177 (2) (1999) 137–159.
[55] S. Shalel, S. Streichman, A. Marmur, Modeling surfactant-induced hemolysis by Weibull survival analysis, Colloids Surf. B 27 (2–3) (2003) 223–229.
[56] G.N. Kumar, U.K. Walle, K.N. Bhalla, T. Walle, Binding of taxol to human plasma, albumin and alpha 1-acid glycoprotein, Res. Commun. Chem. Pathol. Pharmacol. 80 (3) (1993) 337–344.
[57] J. Liu, H. Lee, C. Allen, Formulation of drugs in block copolymer micelles: drug loading and release, Curr. Pharm. Des. 12 (36) (2006) 4685–4701.